# The Design and Operation of Beam Diagnostics for the Dual Stage 4-Grid Ion Thruster

**IEPC-2007-050**

*Presented at the 30th International Electric Propulsion Conference, Florence, Italy*
*September 17-20, 2007*

Cristina Bramanti*
*ESA-ESTEC, Keplerlaan 1, 2201 AZ Noordwijk, The Netherlands*

*and*

David G Fearn†
*EP Solutions, 23 Bowenhurst Road, Church Crookham, Fleet, Hants, GU52 6HS, United Kingdom*

**Abstract:** **In order to increase significantly the specific impulse of a gridded ion thruster, substantially larger ion acceleration potentials are necessary. However, conventional twin- or triple-grid system designs limit this potential to about 5 kV. If 4 grids are utilised, the ion extraction and acceleration processes can be separated, permitting total potentials of up to at least 80 kV to be employed. This concept has been proved in an experimental programme at ESTEC, for which several special diagnostic instruments were designed and built to characterise the high energy ion beam. This paper summarises the performance of the thruster and describes in more detail the results of these diagnostics: a Faraday cup type of ion probe, a shielded Langmuir probe and a calorimeter. In two cases, the performances of these devices within the ion beam are evaluated.**

## I. Introduction

It is now generally recognised that present gridded ion thrusters are limited in their ability to operate at very high values of specific impulse (SI) with a given propellant. This is due to the deeper penetration of the plasma sheath into the discharge chamber plasma as the potential applied between the screen and accelerator (accel) grids is increased to provide greater exhaust velocities. As this penetration extends further into the plasma, the trajectories of many of the extracted ions are changed[1] so that they impact the downstream grids. The resulting sputtering damage reduces thruster lifetime substantially. Although no detailed work has been reported which aims to establish this limit, experience suggests that it is of the order of 5 kV, giving a maximum SI with Xe of about 7500 s, assuming a propellant utilisation efficiency of 85%.

To permit much higher values of SI to be achieved, a dual-stage 4-grid (DS4G) concept has been developed[2], in which the extraction of the ions from the discharge chamber plasma is separated from the acceleration process. Work in the controlled thermonuclear reactor community[3-5] has utilised such systems with total ion accelerating potentials exceeding 80 kV, so there is considerable scope for achieving very high values of SI, should they be required. The high power and thrust densities allow the maximum attainable power for gridded ion engines to be extended from the 40 kW of the present day, to hundreds of kW. This aspect, in combination with the very high specific impulse and a lightweight power system, makes them especially suitable for large, high delta-V future exploration missions, such as interstellar precursors missions, 'delivery and return' cargo transportation of surface

* Research Fellow, Advanced Concepts Team; cristina.bramanti@esa.int.
† Sole Proprietor; dg.fearn@virgin.net.

modules to the low altitude orbits of the Moon and Mars needed for human exploration, or even for an advanced human Mars mission itself [12].

In the space propulsion field, the concept has been verified during an experimental programme at ESTEC[2], in which potentials as high as 30 kV were employed and the SI reached 15,000 s, using Xe. These experiments employed a small low-power experimental laboratory model utilising a radio-frequency (RF) plasma discharge and incorporating various grid designs. During the second phase of this experimental programme, a new set of diagnostic tools was designed and developed, aided by a better understanding of the characteristics of the ion beam. In particular, it was possible to calculate various important plasma parameters within the beam, such as the Debye length and particle mean free paths, with sufficient accuracy to design these diagnostics with some confidence that they would operate successfully over the required ranges of SI, energetic ion current density, and background plasma conditions. Three ion beam diagnostic tools were designed, in addition to an array of Langmuir probes utilised for characterising the ambient discharge chamber plasma. They were:

- A Faraday cup to evaluate the ion density profile in the energetic ion beam, thereby establishing the divergence, which was defined as the half-angle of the cone containing 95% of the energetic ions, and to confirm that the beam was azimuthally symmetrical.
- A calorimeter to determine the power density in the ion beam and validate the results from the Faraday cup.
- A Langmuir probe to determine electron number density and temperature within the beam plasma, and also the plasma potential. The latter was required to identify the degree to which the beam was neutralised.

Clearly, these new diagnostics were specifically designed for making measurements within the very high energy ion beams associated with this new ion thruster. Consequently, they were somewhat novel, since conventional devices are probably unable to provide accurate measurements at such energies and will not survive in this environment due to high rates of sputtering erosion.

This paper, after reviewing the thruster design, performance and operational characteristics presents typical results obtained from two of these diagnostic instruments. These are the Faraday cup and the calorimeter, which were validated during the test campaign and enabled the characterisation of the beam power density and divergence. The results provided a high confidence level regarding the effective design of these diagnostic tools. The Langmuir probe was mounted in the test facility, but it was not possible to perform measurements due to a failure in the data acquisition system which could not be resolved within the time available. Finally the results to characterise the plasma density and electron temperature inside the source tube as function of the RF power and mass flow rate are presented.

## II. The Ion Thruster, Test Facility and Experimental Performance

The proof-of-concept programme, initiated in June 2005, was carried out during two separate test phases, and was performed in the CORONA vacuum facility at ESTEC during November 2005 and May 2006, respectively. Tests were undertaken on a small low-power laboratory model thruster, which was designed and built by the Space Plasma and Plasma Processing Group at the Australian National University (ANU). This work was based on advances made at the ANU concerning RF plasma sources and high voltage electrodes under previous research activities not relating to this project or space propulsion.

### A. The Thruster

A schematic diagram of a thruster employing the dual-stage ion extraction and acceleration process is shown in Fig 1. In this, the discharge chamber can be of any standard design, using RF[6], electron cyclotron resonance[7], Kaufman-type[8] or cusp field ionisation[9] processes. Similarly, the neutraliser system is unchanged from that employed on conventional thrusters.

The only difference is in the grid system configuration and the power supplies connected to the grids. In this case, the positive ions are extracted from the discharge chamber plasma by the electric field applied between the screen and extraction grids. In the work reported here, this

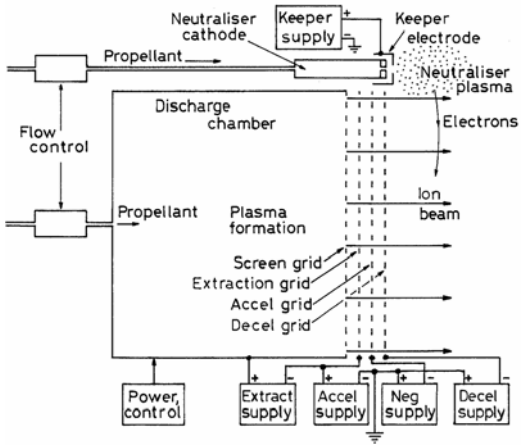


**Figure 1. Schematic diagram of a dual-stage 4-grid ion thruster.**

was limited to a moderate value of below 5 kV to ensure that the distortions to the ion trajectories[1] mentioned above are not a problem. Subsequently, the ions are accelerated to the selected high velocity by the separate field applied between the extraction and accel grids.

The total ion accelerating potential is thus the sum of the extraction and acceleration potentials (Figure 1), and it can be anywhere between 5 and 80 kV, noting that the negative potential applied to the accel grid is not included, since the ions decelerate in passing from this grid, through the decel grid and then entering the space plasma. This negative potential is necessary to prevent electron backstreaming into the thruster from this external plasma. As well as decelerating the primary ions, the external decel grid absorbs charge-exchange ions originating in this plasma, thereby partially protecting the accel grid from erosion.

The experimental laboratory thruster is shown in a sectional view in Fig 2, with the gas inlet at the top and the grid assembly at the bottom. A photograph is presented in Fig 3, in which the edges of the grids can be seen at bottom right. The device was based on a 5 cm diameter cylindrical discharge chamber made from ceramic and fed with a regulated flow of Xenon gas, although the active area of the grids was restricted to about 2 cm to ensure an approximately uniform plasma density across the grid apertures.

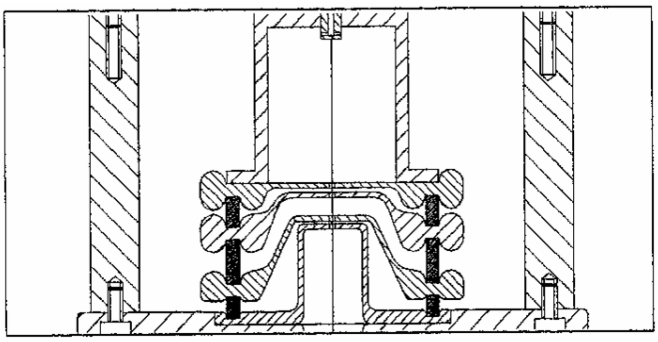

**Figure 2. Sectional view of the experimental thruster.**

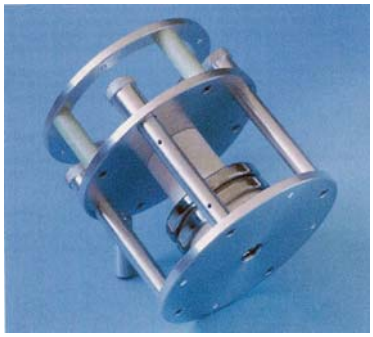

**Figure 3. Photograph of the ion thruster.**

The RF discharge was energised by a 3-turn antenna coiled around the discharge chamber, and biased to the screen grid voltage (this is not shown in Figures 2 and 3). This antenna was fed from a manually-tuned RF system operating at 13.56 MHz. The 4-grid system, connected to appropriate power supplies, was attached to the discharge chamber using the clamping arrangement shown in Fig 2. Under suitable conditions, this resulted in the desired highly focused energetic ion beam.

### B. The Test Facility

The DS4G thruster was mounted inside the CORONA facility's secondary chamber, which has dimensions of 1m diameter and 1 m length. The main chamber is of 2 m diameter and 4 m length. Vacuum levels of down to $10^{-8}$ millibars were attained in the facility. The gate valve between the two chambers was opened to allow the ion beam to travel 4 m into a large volume before colliding with the graphite target. No active neutraliser was used in the experiments; hence any neutralisation of the beam was by secondary electron emission from the target.

Diagnostic equipment was mounted on motorised arms, which were swept over wide angles in two perpendicular directions in the main vacuum chamber. Measurements were taken of the ion beam at a distance of 1.5 m from the thruster exit plane. During the first phase of the programme, the following existing diagnostic tools were used:

- A single-electrode Langmuir probe, which gave the electron temperature and potential of the plasma surrounding the beam (not within the beam).
- A simple Faraday cup, which provided an indication of the ion current density in the beam.
- Electrostatically-biased wire electrodes, which provided a measure of beam divergence. This was calculated to include 95% of the collected current to the wires, integrated over the angle from the thruster bore axis.

The Faraday cup unfortunately did not provide satisfactory results, probably due to a non-optimised design. In addition, during each test, thruster operating data were acquired and recorded continuously; the parameters measured included grid currents and voltages, as well as propellant flow rate and RF power. During the second phase of the programme, the new beam diagnostic tools provided more accurate beam measurements. .

### C. First Test Phase Results

Prior to attempting beam extraction from the DS4G laboratory thruster, thermal and high voltage breakdown tests were performed. The thruster was able to operate with an RF plasma discharge at power levels of up to 600 W for over 45 minutes, significantly beyond the anticipated 10-15 minutes beam tests, thus giving good margins and confidence in the RF subsystem. Breakdown tests were run with voltages on the first two grids reaching 30 kV and 27 kV respectively in vacuum conditions, providing confidence in the HV subsystem operation.

The principal aims and achievements of the first test phase were:

i. To demonstrate the theoretical performance expected of a dual-stage 4-grid ion extraction/acceleration system operating at beam potentials of up to 30 kV with xenon propellant, notably very high values of SI, and of power and thrust densities. These objectives were initially achieved with a single aperture four electrode (SAFE) configuration, with a single 1 mm diameter aperture. This was changed later to a 4-grid system containing 43 apertures of 1 mm diameter, which provided a considerably enhanced beam current.

ii. To characterise the extracted ion beam and overall performance with variations of plasma density, ion extraction potential and beam acceleration potentials. Performance data are summarised below, and the beam divergence of typically less than 5° was well below any values recorded for other ion thrusters.

iii. To attempt to optimise the ion optics by minimising grid impingement currents. This was done by varying extraction potential, discharge power and xenon flow rates. The results were ambiguous due to deficiencies in the design of the thruster.

Table 1 presents the operating parameters obtained from a typical experimental test run, and the best values achieved. The data for the typical test are related to a beam potential of 25 kV. The programme was a remarkable success and the DS4G concept was proved to work in practice, in the context of space propulsion, for the first time. The thruster was able to operate at beam potentials of up to 30 kV and produced an excellent performance in terms of SI, thrust density and power density (based on grid open area), and beam divergence. The values achieved represent an improvement by several times on the current state-of-the-art, whilst maintaining very small direct ion impingement of the beam on the grids.

**Table 1. Summary of DS4G laboratory model performance during the first phase of the experimental campaign at ESTEC, performed in November 2005.**

| Performance Parameters | Typical Value | Best Value | Operating Parameters | Range |
|---|---|---|---|---|
| Thrust (mN) | 2 | 2.85 | Beam potential (kV) | 10 - 30 |
| Specific impulse (s) | 14,000 | 15,000 | Extraction potential (kV) | 3 - 6 (3 optimum) |
| Total efficiency | 0.34 | 0.34 | Beam current (mA) | 4 - 12 |
| Mass utilisation efficiency | 0.73 | 0.75 | Beam power (W) | 100 - 260 |
| Electrical efficiency | 0.47 | 0.47 | RF power (W) | 100 - 490 |
| Beam divergence (deg) | 5 | 2.5 | RF plasma density ($cm^{-3}$) | $2.5 \times 10^{11} - 1.23 \times 10^{12}$ |
| Grid impingement (%) | 2 | 1 | Xe mass flow rate (mg/s) | 0.004 - 0.014 |
| Open area thrust density ($mN/cm^2$) | 5.9 | 8.4 | Beam diameter (cm) | 2.3 |
| Open area power density ($W/cm^2$) | 555 | 740 | Grid open area ratio (%) | 8.1 |
| Total thrust density ($mN/cm^2$) | 0.5 | 0.7 | Beam plasma electron temp (eV) | 5.7 - 11.0 (± 0.5) |
| Total power density ($W/cm^2$) | 45 | 60 | Beam plasma potential (V) | 24 - 52 (± 2) |

The thruster utilised in this first phase of the project was designed with one objective in mind, namely to prove the feasibility of the operation of the 4-grid concept at high beam potentials. Thus the grid ion optics were not optimised and the open area ratio was very low, leading to a low extracted beam power compared to the RF power input. Therefore, the electrical efficiency, and hence the total efficiency, achieved by the thruster were low, even when the propellant utilisation efficiency was relatively high at over 70%. The need to remedy this situation led to the design of the device tested in the second phase of the project.

**D. Second Test Phase Results**

From analyzing the results obtained from the first test phase, the need to improve total efficiency to typical gridded ion thruster levels before a flight engineering model suitable for spacecraft applications could be contemplated was evident (no requirement was originally set for this parameter). This led to the initiation of a second experimental test phase utilising a revised grid optics design, with a considerably increased open area ratio of 61% (Figure 4). This design was based on well-established ion thruster grid system principles, modified as necessary to accommodate the 4th grid. The main objectives of the second test phase were:

i. To validate experimentally the new grid ion optics design in order to improve the efficiency of the thruster to values similar to or greater than those of conventional ion thrusters.

ii. To characterise and refine the performance of the thruster with the new grid sets, at different operating points (defined by beam current and beam accelerating potential), with xenon propellant.

iii. To characterise the ion beam optics (in terms of grid impingement, beam divergence and beam plasma parameters) and extracted beam current density, for each of the test configurations and operating points.

iv. To characterise the plasma density in the source tube as a function of the RF power, mass flow rate and radial position in order to improve the knowledge of conditions close to the plasma sheath.

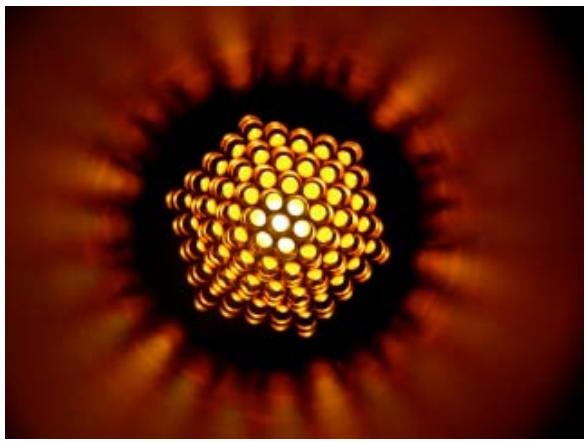

**Figure 4. Thruster screen grid with open area ratio of 61%.**

Prior to the start of the second test programme in May 2006, simulations of the new design verified the revised ion optics approach and predicted that much higher beam currents could be achieved for the same RF power, due to a grid extraction area over 5 times larger, or conversely the use of a much lower RF power for the same beam power. Table 2 presents operating parameters from the second test phase; this provides one set of results obtained during a typical test run, and the best values achieved.

Due to the introduction of the new ion optics, higher values of electrical efficiency and total efficiency, as well as total thrust and power density, were reached. The mass utilisation efficiency improved from 70% to between 80-96% by optimising the beam current in relation to the mass flow rate. This improvement contributed to an increase in the total efficiency to 70% in some cases, similar to that achieved in conventional gridded ion thrusters.

It should also be pointed out that these data are pessimistic, because they assume that all currents collected by the extraction and accelerator grids were due to direct ion impingement. As a consequence, these grid currents were subtracted in full from the beam current, as deduced from the electron current to the screen grid, to give a reduced beam current. This was utilised in calculating thruster performance parameters. In reality, it is not possible with the available data to assess the actual impingement currents, because the current flow to each grid was a combination of particle fluxes from a variety of sources. These were the charge-exchange ions formed within the grid system, secondary electrons produced by ion impact, particles collected from the external plasma, and the direct ion impingement itself. Thus values derived ignoring the currents to the extraction and accelerator grids would be optimistic, and would represent the maximum possible performance in the absence of direct impingement.

This additional assessment was made and, as predicted, the derived performance increases significantly, to typically 3.7 mN at the nominal 2.7 mN thrust level, and to 6.75 mN at 5.4 mN.

It should also be pointed out that there is some uncertainty regarding the values of propellant utilisation efficiency derived from the mass flow rate data. This is because, owing to lack of time, it was not possible to allow the thruster to stabilise fully after altering operating conditions before taking data. So, although the flow controller was accurate, the pressure distribution within the feed system and the thruster had not necessarily reached complete equilibrium, despite a typical test run lasting for 10 to 15 minutes. To assess accurately the degree of uncertainty resulting from this departure from steady-state is not simple, since it includes, for example, the way in which the ionisation processes within the discharge chamber responded to pressure changes, but a preliminary assessment suggests that 5% may be a realistic figure.

**Table 2. Summary of DS4G laboratory model performance during the second phase of the experimental campaign at ESTEC, performed in May 2006.**

| Performance Parameters | Typical Value | Best Value | Operating Parameters | Range |
|---|---|---|---|---|
| Thrust (mN) | 2.7 | 5.4 | Beam potential (kV) | 10 – 17.5 |
| Beam potential (kV) | 15 | 17.5 | Extraction potential (kV) | 1.5 – 5 |
| Specific impulse (s) | 14000 | 14500 | Screen grid (beam) current (mA) | 4 -33 |
| Mass utilisation efficiency | 0.96 | 0.96 | RF power (W) | 20 – 316 |
| Electrical efficiency | 0.66 | 0.75 | Beam power (W) | 80-398 |
| Total efficiency | 0.63 | 0.7 | Total efficiency | 0.4-0.7 |
| Beam divergence (deg) | 4.6-5.3 | 3.8 | Electrical efficiency | 0.5-0.75 |
| Total power (W) | 300 | 614 | Beam divergence | 3.8-6.2 |
| RF power (W) | 101 | 316 | Xe mass flow rate (mg/sec) | 0.01 - 0.05 |
| Total thrust density (mN/cm$^2$) | 0.86 | 1.7 | Beam diameter (cm) | 2 |
| Total beam power density (W/cm$^2$) | 64 | 126 | Grid open area ratio | 61 % |

## III. Plasma and Ion Beam Conditions

A critical parameter in designing many plasma diagnostic instruments is the Debye length, $\lambda_D$. This is the electrostatic shielding distance, and gives an indication of the dimensions over which the plasma will not be influenced by an imposed electric field. It is thus important in deciding the maximum permissible orifice diameter of an ion probe, in which the potential of the orifice plate is relied upon to exclude external electrons. It also determines the minimum size of a Langmuir probe, if thin sheath theory is to be applied to the data acquired by such a device; basically, the probe must be much larger than $\lambda_D$. But for the beam divergence, the Debye length, $\lambda_D$, in the ion beam emanating from the thruster would be easy to calculate. However, due to the expansion of the beam as it moves away from the thruster, the electron number density, $n_e$, falls and $\lambda_D$ increases. The latter point can be seen from the equation for $\lambda_D$, which is, using CGS/electrostatic units[10],

$$\lambda_D = \left( \frac{kT_e}{4\pi e^2 n_e} \right)^{1/2} = 6.9 \left( \frac{T_e}{n_e} \right) \text{ cm} \qquad (1)$$

Here, $T_e$ is the electron temperature, $k$ is Boltzmann's constant and $e$ is the charge on an electron.

In evaluating $\lambda_D$, it was assumed from the first phase of the programme that $T_e$ is about 5 eV, and that this is approximately independent of thruster operating conditions.

The results of these calculations are shown in Figure 5, assuming that the probe is situated 100 cm from the thruster exit plane. Data are given for a maximum beam current of 80 mA, an arbitrary intermediate value of 10 mA, and a lower value of 1 mA, beneath which there is unlikely to be any interest in the performance of the thruster. The values of $\alpha$ plotted fall in the range 0.5 to 2.5°, and the ion beam accelerating potential has been assumed to be 30 kV. One curve for 20 kV and 80 mA is also shown, which suggests that the dependence of $\lambda_D$ on $v_i$ is not great.

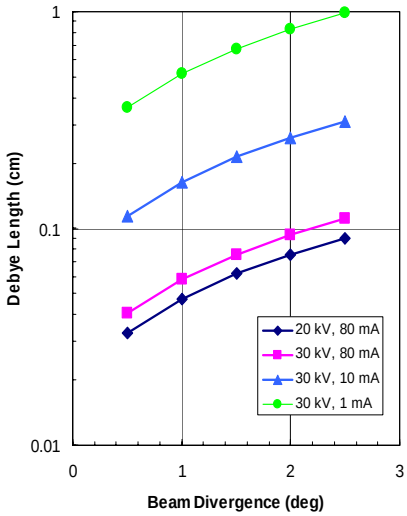


**Figure 5. Debye length in the ion beam as a function of divergence and beam current.**

In order to estimate the likely responses of given designs of ion probe and Langmuir probe to the ion beam and associated embedded plasma, estimates of $n_e$ and $n_i$ were required. Assuming that the ion beam was fully neutralised, and that the plasma associated with it was also electrically neutral, these

parameters were taken to be identical. These values, together with $\lambda_D$ from Figure 5, were utilised in determining the size of the Langmuir probe, then for calculating its sensitivity.
Other very important criteria were determined by these parameters, all of which were evaluated theoretically by Spitzer[10]. As an example, the sweep rate of the potential applied to a single Langmuir probe must be sufficiently slow for the plasma being monitored to remain in equilibrium throughout; thus this rate must be much slower than the time required for particle anisotropies to be removed by collision processes.

## IV. The Faraday Cup Ion Probe

The ion beam profile was measured at a distance of 1.5 m from the thruster using a Faraday cup probe. This probe was designed using conventional principles, although care had to be exercised in accounting for the high ion beam energy. In principle, both energetic and slow ions were permitted to enter the device through the central orifice, being attracted by its negative potential. Conversely, electrons were excluded by this potential.

A picture of the probe mounted inside the movable arm is presented in Figure 6, while Figure 7 shows the high energy ion beam produced by the thruster (emanating from the right hand side of the picture) and beam characteristics being measured by the dedicated intrusive diagnostics which can be seen on the left.

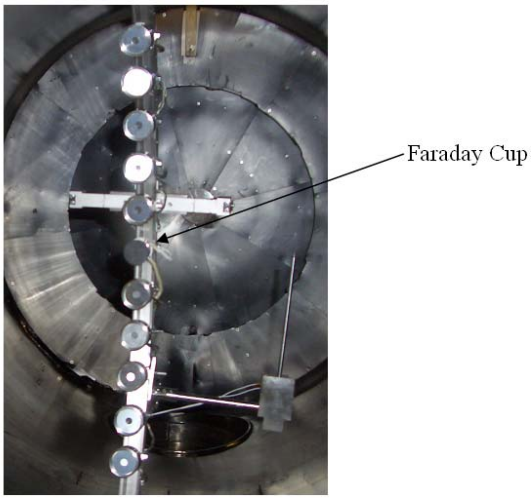


**Figure 6. Faraday cup ion probe mounted on the movable arm.**

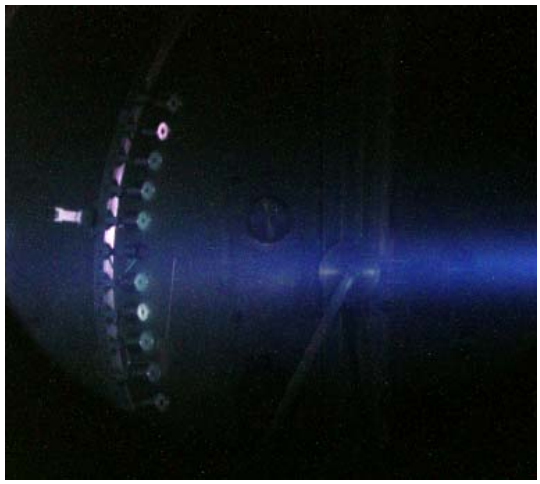

**Figure 7. High energy beam produced by the thruster and the faraday cup arm on the left.**

Typical results are shown from Figure 8 to Figure 11, while Table 3 presents the divergence values derived from several tests performed in different test conditions. The actual beam current within each radial position is plotted against the sweep angle. The beam divergence was derived from these plots; it was defined as the beam half-angle containing 95% of the total beam current. As can be seen, the values of divergence were very low, which is far better than ever recorded with a conventional ion thruster.

The shape of this curve is representative of the bulk of the acquired data and confirmed that the ion beam was azimuthally symmetrical, as anticipated. Bearing in mind the very low current density at this distance from the thruster and the electrical noise present, these curves are very smooth and symmetrical, and can be regarded as fully satisfactory. Although it has not been possible so far to correlate this shape with the detailed ion optics, this should eventually be possible. As intended in the design, noise was generally absent from the data, aiding interpretation.

**Table 3. Summary of some divergence values obtained by the Faraday cup measurements in different test conditions (mass flow rate, RF power, extraction potential and screen grid potential) during the second phase of the experimental campaign at ESTEC, performed in May 2006.**

| Beam Test | Mass Flow Rate (mg/sec) | Screen Grid Voltage [kV] | Extraction Potential [kV] | RF [W] | Divergence [deg] |
|---|---|---|---|---|---|
| 24 | 0.03 | 10 | 1.5 | 20 | 5 |
| 29 | 0.015 | 10 | 3 | 50 | 4.5 |
| 32 | 0.01 | 10 | 3 | 60 | 4.7 |
| 42 | 0.02 | 15 | 2.5 | 60 | 3.6 |
| 43 | 0.02 | 15 | 5 | 60 | 5.1 |
| 45 | 0.02 | 17.5 | 5 | 60 | 5.3 |
| 46 | 0.02 | 15 | 5 | 150 | 4.3 |
| 47 | 0.02 | 15 | 5 | 50 | 5.2 |

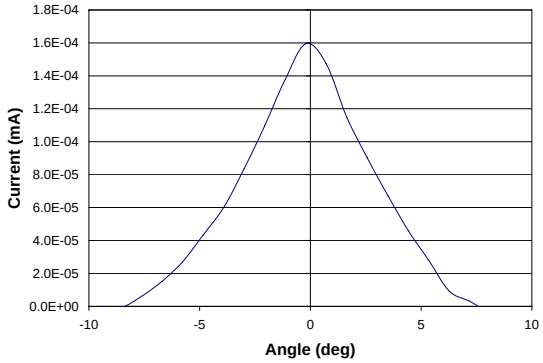


**Figure 8. Beam profile test #24 (mass flow rate = 0.03 mg/sec, RF power = 20 W, $V_1$ = 10 kV and $V_2$ = 8.5 kV). Derived beam divergence = 5 deg.**

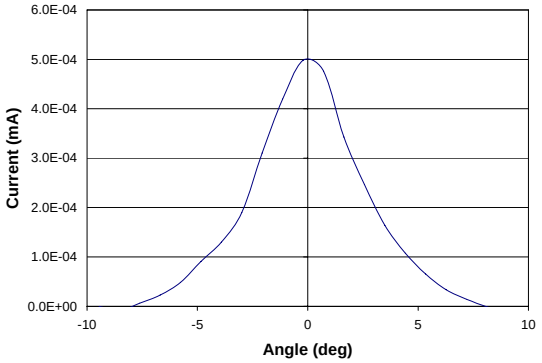


**Figure 9. Beam profile test #32 (mass flow rate = 0.01 mg/sec, RF power = 60 W, $V_1$ = 10 kV and $V_2$ = 12 kV). Derived beam divergence = 4.7 deg.**

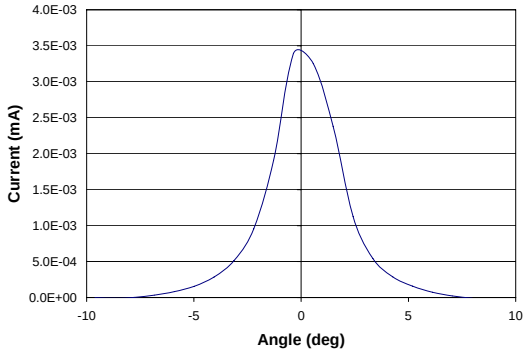


**Figure 10. Beam profile test #42 (mass flow rate = 0.02 mg/sec, RF power = 60 W, $V_1$ = 15 kV and $V_2$ = 12.5 kV). Derived beam divergence = 3.6 deg.**

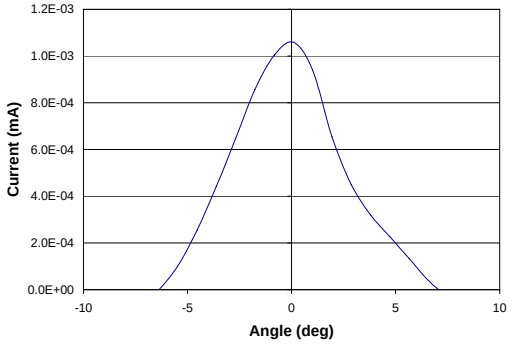


**Figure 11. Beam profile test #46 (mass flow rate = 0.02 mg/sec, RF power = 150 W, $V_1$ = 15 kV and $V_2$ = 10 kV). Derived beam divergence = 4.3 deg.**

Table 3 confirms that one important parameter which influences the divergence value is the extraction potential. For example, during the tests #42 and #43, which were performed at the same RF power, screen grid potential and mass flow rate, but with different extraction potential, the divergence has much lower value when the extraction potential is lower. This fact outlines the necessity to optimize the extraction potential in order to finally optimize the thruster overall efficiency. During the tests due to the lack of time it was not possible to perform a full optimization for each screen grid potential value.

It was concluded that the probe design was satisfactory and that it operated as expected in a very hostile environment. Although long duration tests were not possible, damage was negligible, validating the decision of using durable materials for the components exposed to the high energy beam.

## V. The Calorimeter

This device, mounted on the movable arm, was intended to measure the power density as a function of position in the ion beam (Figure 12).

The operation of this device was very simple. The entrance aperture defined a portion of the ion beam which was allowed to enter the instrument and impacted upon a target. The energy deposited within this assembly by the beam caused a temperature rise, which was sensed by a thermocouple.

It was intended to scan the device across the ion beam at a constant velocity, using the probe carriage mentioned previously. In this case, the measured temperature rise would give an immediate indication of the total input energy from a section of the beam defined by the entrance aperture. This could then be related to the total energy in the beam. Such a test could also give confirmation of the beam divergence, if scanned very slowly. Unfortunately, time constraints did not permit these more complex uses to be implemented.

In general use, the time for which heating occurred was determined by the width of the ion beam and the sweep speed of the probe carriage. As mentioned above, it was anticipated that virtually all the kinetic energy of the ion beamlet entering the collector was deposited within it, so the temperature rise, of only a few degrees, gave a measure of the total energy.

On a longer timescale, radiative and conduction losses might have caused the temperature to reach a plateau. However, this was not considered to be a significant limitation, since these losses were very small with a temperature difference of only a few degrees.

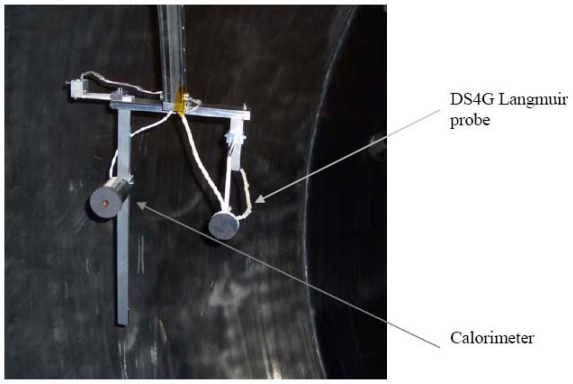


**Figure 12. Calorimeter and Langmuir probe mounted in the vacuum test facility**

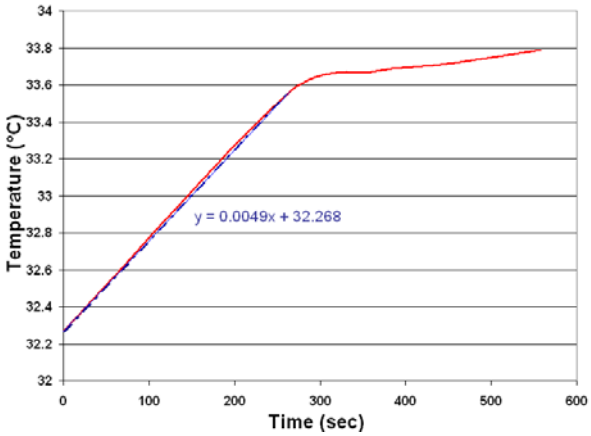


**Figure 13. Typical calorimeter temperature profile as function of the time.**

A typical result with the calorimeter stationary in the centre of the beam is presented in Figure 13. In this case the conditions included a beam current of 20 mA, an ion extraction potential of 5 kV, and a total accelerating potential of 15 kV. As can be seen, the thermocouple indicated that the collector temperature rose linearly with time until the device was removed from the beam.

The derived beam power density in this case

was 0.147 W/cm$^2$. In order to verify the validity of the measurement, this result was compared with the peak beam power density measured by the Faraday cup in the same test, which resulted to about 0.15 W/cm$^2$. Bearing in mind the loss of ions due to charge-exchange processes external to the thruster, which would not have been detected by the ion probe, these results provided confirmation of the effective design of these diagnostic tools.

## VI. Discharge chamber Langmuir Probes

The electron temperature, number density and plasma potential of the discharge plasma inside the source tube have been obtained through measurements performed by five thin single-electrode Langmuir probes inserted through the first grid into this tube. This allowed the evaluation of the plasma density distribution across the full diameter of the grid. Several tests were performed on the 5 probes at different flow rates and RF power levels by sweeping the voltage between the probe and the reference potential surface from a negative to positive values, and the Langmuir probe characteristics have been derived and analysed. This investigation of plasma parameters within the discharge chamber of the DS4G thruster was successful because it confirmed that both electron temperature, $T_e$, and number density, $n_e$, are within the ranges originally predicted at the outset of this research programme. It was found that $T_e$ is consistently within the range 2 to 5 eV. These values are fully acceptable and are consistent with the plasma under study. As expected, there is some evidence that $T_e$ increases with RF power, but this was not found under all circumstances.

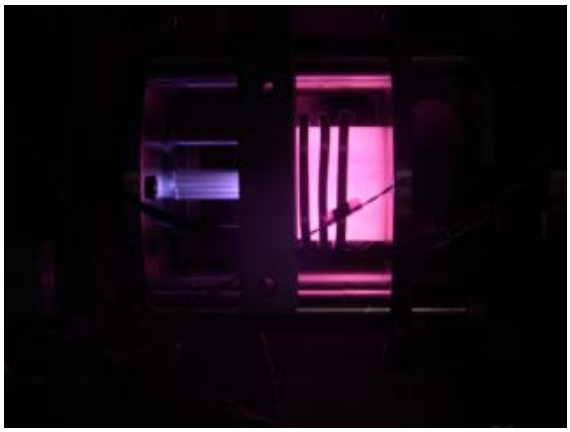

**Figure 14. The DS4G during the experiment with the Langmuir probes inserted in the discharge chamber**

Similarly, the number density was within the anticipated range, 4 to $25\times10^{11}$ cm$^{-3}$. It was notable that the highest values, of above $20\times10^{11}$ cm$^{-3}$, did not appear until the flow rate was increased to 0.08 mg/s; below that figure, $n_e$ never exceeded $12\times10^{11}$ cm$^{-3}$. Thus it can be concluded that the number density was an extremely non-linear function of flow rate, but the exact form of this relationship remains to be determined. The values of $n_e$ derived from these probes were internally consistent, although there was evidence that the second probe, adjacent to the central one, was recording relatively low ion currents; this may well have been due to a slightly smaller active area. It was concluded that the plasma density profile was relatively flat, with a central peak that was approximately up to 15 to 20 % above the values at the edges of the grids.

The derived values of the electron temperature and number density at three different RF power levels and at a flow rate of 0.02 mg/sec are presented in Table 4. The results at 150 W were particularly difficult to assess, due to serious oscillations in the characteristics, which was almost certainly an artefact of the automated voltage sweep system employed. As a consequence, the temperatures for probes L2, L3 and L4 fell within the range indicated for L1/L5; the mean was used for the former probes. Some analysis errors were assessed and they are of the order of 0.5 eV for $T_e$ and about 10 to 15 % for $n_e$.

**Table 4. Electron temperature and plasma density inside the source tube for several RF power values and a flow rate of 0.02 mg/sec.**

| Power (W) | 50 | | 100 | | 150 | |
|---|---|---|---|---|---|---|
| | $T_e$ (eV) | $n_e$ ($10^{12}$cm$^{-3}$) | $T_e$ (eV) | $n_e$ ($10^{12}$cm$^{-3}$) | $T_e$ (eV) | $n_e$ ($10^{12}$cm$^{-3}$) |
| L1/L5 | 4.95 | 0.590 | 5.15 | 0.629 | 6.85/4.26 | 0.836 |
| L2/L4 | 4.94 | 0.541 | 4.67 | 0.580 | (5.56) | 0.717 |
| L3 | 4.28 | 0.733 | 5.59 | 0.694 | (5.56) | 0.819 |

With a current sensing resistor of 5 kΩ, it is clear that the ion saturation currents were reasonable, as were the equivalent potentials; they should have enabled appropriate values of $n_e$ to be obtained. Similarly, the values of the electron saturation current were acceptable, but the equivalent voltages were far too high at the larger plasma densities. However, as only the start of the electron retarding region is required from a probe characteristic to obtain $T_e$, it was deemed preferable to restrict the range of the sweep of probe potential to avoid entering this high current region. Indeed, the electron saturation region is usually poorly defined in a Langmuir probe characteristic, so its loss was of no great consequence.

## VII. Conclusions

This paper has summarised a very successful two-phase experimental campaign to validate the concept of the Dual-Stage 4-Grid ion thruster, in which the ion extraction and acceleration processes are separated. This removes a major limitation inherent in the traditional twin- and triple-grid systems, which normally prevents total accelerating potentials from rising much above 5 kV.

This experimental programme utilised a small low-power laboratory model thruster, in which a radiofrequency discharge was used to provide the plasma for the ion beam. Total accelerating potentials of up to 30 kV were demonstrated. Unprecedented narrow beam divergences of the order of 2° to 5° were also achieved. The SI reached about 15,000 s using Xenon propellant, and open area thrust and power densities of 8.4 mN/cm$^2$ and 740 W/cm$^2$, respectively, were attained. In the second phase of the programme, total efficiencies of 70% and values of thrust of over 5 mN were achieved due to the introduction of a revised grid design with a much increased open area ratio.

In the second phase of the work, specially designed diagnostic tools were produced for characterising this highly energetic ion beam. These consisted of a Faraday cup ion probe, a calorimeter and a shielded Langmuir probe. The operation of two of these devices has been described; these are the ion probe and the calorimeter. Unfortunately, problems with other parts of the experimental apparatus prevented tests with the Langmuir probe from being carried out. Nevertheless, the ion probe was found to operate as designed and enabled characterisation of the ion flux in the beam as a function of angle, and thus derivation of the beam divergence. The calorimeter also operated successfully, and allowed the power density in the beam to be determined independently. The experiment performed with five Langmuir probes inserted inside the discharge chamber allowed the estimation of the electron temperature and plasma density of the discharge chamber, and its distribution over the full grid diameter.

These results are most encouraging, and pave the way for future work to further develop the basic concept. Characterisation of the ion beam would not have been possible without these new diagnostic tools and it is anticipated that they could be exploited further for performance and lifetime optimization in any future development programme of a flight engineering model DS4G ion thruster.

## Acknowledgments

The authors would like to acknowledge the technical staff at ANU, Dr Orson Sutherland, Professor Rod Boswell, Dr Christine Charles, Peter Alexander and Dennis Gibson, who built the laboratory model thruster. The authors also express their gratitude to Dr Jose Gonzalez, Mr Pierre Frigot and Ms Marika Orlandi from the ESTEC Electric Propulsion Laboratory for their support during the experimental campaign, and to Dr Franco Ongaro, Dr Giorgio Saccoccia, Dr Leopold Summerer, Mr Andrés Gálvez, Mr Bruno Sarti, Mr Philippe Meijgaarden and the Workshop team from ESA for their continuous support and encouragement.

*This paper is published in the memory of David Fearn, who sadly died on 29 August 2007 before being able to present the work at the IEPC conference. He will be greatly missed by me, his many friends, collaborators and colleagues in the electric propulsion community to which he gave so much.*

## References

[1] Fearn, D G, "The application of gridded ion thrusters to high thrust, high specific impulse nuclear-electric missions", IAF Paper IAC-04-R.4/S.7.09, (October 2004). *J Brit Interplan Soc*, **58**, 7/8, 257-267, (July/August 2005).

[2] Walker, R, Bramanti, C, Sutherland, O, Boswell, R, Charles, C, Fearn, D, Gonzalez, J, Frigot, P and Orlandi, M, "Initial experiments on a dual-stage 4-grid ion thruster for very high specific impulse and power", AIAA Paper 2006-4669, (July 2006).

[3] Martin, A R, "High power beams for neutral injection heating", *Vacuum*, **34**, 1-2, 17-24, (1984).

[4] Okumura, Y, et al, "Quasi-dc extraction of 70 keV, 5 A ion beam," *Rev Sci Instrum*, **51**, 728-734, (1980).

[5] Menon, M M, et al, "Power transmission characteristics of a two-stage multiaperture neutral beam source," *Rev Sci Instrum*, **51**, 1163-1167, (1980).
[6] Killinger, R, Bassner and H, Müller, J, "Development of an high performance RF-ion thruster", AIAA Paper 2000-2445, (July 2000).
[7] Kuninaka, H, Funaki, I, Nishiyama, K, Shimizu, Y and Toki, K, "Result of 18,000-hour endurance test on microwave discharge ion thruster", AIAA Paper 2000-3276, (July 2000).
[8] Fearn, D G and Smith, P, "A review of UK ion propulsion -a maturing technology", IAF Paper IAF-98-S.4.01, (Sept/Oct 1998).
[9] Christensen, J A et al (12 authors), "Design and fabrication of a flight model 2.3 kW ion thruster for the Deep Space 1 Mission", AIAA Paper 98-3327, (July 1998).
[10] Spitzer, L, Jnr, "Physics of fully ionized gases", Interscience Publishers Inc, NY and London, (1961).
[11] Glasstone, S and Lovberg, R H, "Controlled thermonuclear reactions", van Nostrand, (1960), pp 194-202.
[12] Bramanti, C., Walker, R., Izzo, D., Fearn, D.G., Samaraee, T., "Very High Delta-V Missions to the Edge of the Solar System and Beyond Enabled by the Dual-Stage 4-Grid Ion Thruster Concept", *Proceedings 57th International Astrodynamics Conference,* paper IAC-06-D.2.8.3, 2006.